MOLECULAR PHYSICS REPORTS **40** (2004) 95-103

SIZE-INDUCED LOCALIZATION OF QUANTIZED MAGNETOSTATIC MODES IN DIPOLAR NANOCUBES

M. KRAWCZYK[1], H. PUSZKARSKI[1], AND J.-C. S. LÉVY[2]

[1]*Surface Physics Division, Faculty of Physics, Adam Mickiewicz University*
Umultowska 85, 61-614 Poznań, Poland

[2]*Laboratoire de Physique Théorique de la Matière Condensée, case 7020*
Université Paris 7, 2 place Jussieu, 75251 Paris Cédex 05, France

Abstract. We investigate the dynamical properties of a system of interacting magnetic dipoles disposed in sites of an *sc* lattice and forming a cubic-shaped sample. The applied magnetic field is assumed to be oriented along the central axis connecting opposite cube face centers, magnetizing uniformly the whole sample, all the dipoles being aligned parallelly in the direction of the applied field. The frequency spectrum of magnetostatic waves propagating in the direction of the applied field is found numerically by solving the Landau-Lifshitz equation of motion; the mode amplitude spatial distributions (*mode profiles*) are depicted as well. It is found that only the two energetically highest modes have *bulk-extended* character. All the remaining modes are of *localized* nature; more precisely, the modes forming the lower part of the spectrum are localized in the *subsurface region*, while the upper-spectrum modes are localized around the sample center. We show that the mode localization regions narrow down as the cube size increases and in sufficiently large cubes one obtains practically only *center-localized* and *surface-localized* magnetostatic modes.

1. The development of nanotechnology in recent years allowed to design nanometric ferromagnetic materials of any required shape with a large size variation range [1]. Small magnets and particles have raised an increasing interest due to their potential application in magnetic random access memory (MRAM) elements and ultrahigh-density storage. This interest also involves the sample ability to rapidly change the magnetization state in order to optimize the individual recording time. Particularly, magnetostatic modes are of practical importance in this matter (especially in magnetization reversal processes), by reason of their low frequency range.

The localized magnetostatic mode dynamics has been investigated by several authors. Berkov *et al*. [8] studied the spin wave frequency spectrum and spatial distribution in thin μm-sized magnetic film samples. The lowest-frequency modes were found to correspond to oscillations restricted to the boundary regions, which start to "propagate" inside a rectangular magnetic sample as the frequency increases. Tamaru et al. [3] applied a spatially resolved FMR technique to quantized magnetostatic mode imaging in small magnetic structures. They identified quantized magnetostatic modes in the obtained spectra, and from the observed spatial distribution of magnetization response at each mode peak deduced that the number of mode nodes decreased with increasing bias field. However, in their data interpretation some discrepancies were found between the measured mode frequency values and those calculated on the basis of the Damon-Eshbach theory [4]. An exact theory of spin wave mode quantization in small magnetic structures needs to be developed.

Our theoretical approach is based on a modified Draaisma-de Jonge treatment [5] used in the dipolar energy calculation. In the original Draaisma-de Jonge treatment a ferromagnetic film is considered as a set of discrete magnetic dipoles regularly arranged in a crystalline lattice. The dipolar energy is calculated by collecting contributions from each dipolar lattice plane assumed to be parallel to the film surface. The dipoles within each plane are divided into two sets: those within a circle of radius R and those beyond that circle; the total contribution of the former set is calculated discretely through summing over the dipoles, while the contribution of the latter set is evaluated by integration (the circle radius should be large enough to assure reliable final results). In the approach used in our study, the discrete summation is performed over *all* the dipoles within a given dipolar plane; thus, the integration is avoided, and no approximation is involved in our dipolar energy evaluation.

2. We shall consider a system of magnetic moments $\vec{\mu}_r$ arranged regularly in sites r of a simple cubic crystal lattice. The system is assumed to form a rectangular prism with square base (see Fig. 1a). Let the prism base determine the (x, y)-plane of a Cartesian reference system, with the z-axis perpendicular to this plane. The reference point (0, 0, 0) shall be placed in the *central site* of the prism bottom.

Let us calculate magnetic field $\vec{h}_R$ "produced" by all the prism dipoles in a site indicated by internal vector R. According to the classical formula (obtained using the linear approximation), field $\vec{h}_R$ can be expressed as follows (in the SI units):

$$\vec{h}_R = \frac{1}{4\pi} \sum_{r \neq R} \frac{3\left(\vec{r}-\vec{R}\right)\left(\vec{\mu}_r \cdot \left(\vec{r}-\vec{R}\right)\right) - \vec{\mu}_r \left|\vec{r}-\vec{R}\right|^2}{\left|\vec{r}-\vec{R}\right|^5} . \tag{1}$$

the above sum involving all the sites *except* the reference point (*i.e.* the site with position vector $r \equiv R$). The lattice planes parallel to the prism base shall be numbered with index $n = 0, N-1$ (see Fig. 1b), and the sites within each plane indexed with vector $r_p = a\left[p\hat{i} + q\hat{j}\right]$, defined by integers $p, q = -L, L$. This means that the position of the sites in which the magnetic moments are located, indicated by vector r, shall be defined by a set of three integers, (p, q, n):

$$r \equiv \left[r_p, an\right] \equiv a[p, q, n], \quad p, q \in \langle -L, +L \rangle \quad \text{and} \quad n \in \langle 0, N-1 \rangle , \tag{2}$$

a denoting the lattice constant. Thus, the considered prism contains $N(2L + 1)^2$ magnetic moments. Below we shall focus on the magnetic field on the z-axis only, assuming its direction to be solely allowed for magnetic wave propagation. Hence, we put $R \equiv a[0, 0, n']$, where $n' = 0, N-1$, and re-index the dipole field: $h_{n'} \equiv \vec{h}_R$. Additionally, we shall assume that all the magnetic moments within *a single plane n* are identical, *i.e.*:

$$\mu_n \equiv \mu_{[p,q,n]}, \quad \text{for any } p \text{ and } q. \tag{3}$$

Note that by assuming $\mu_n \equiv \vec{\mu}_r$ all the magnetic excitations propagating in *plane* (x, y) are excluded from our analysis, and z axis becomes the only direction of propagation allowed.

In order to obtain a simpler expression of $h_{n'}$ we introduce a symmetric matrix whose elements, $D_{n,n'}$, are defined as follows:

$$D_{n,n'} = \sum_{p,\,q} \frac{\frac{1}{2}\left(p^2+q^2\right)-\left(n-n'\right)^2}{\left[p^2+q^2+\left(n-n'\right)^2\right]^{5/2}}\,. \tag{4}$$

With this matrix, the magnetic field reads:

$$\vec{h}_{n'} = \frac{1}{4\pi}\sum_n \left[D_{n,n'} \frac{\hat{i}\,\mu_n^x + \hat{j}\,\mu_n^y - 2\hat{k}\,\mu_n^z}{a^3} \right]. \tag{5}$$

It is convenient to introduce here the notion of *magnetization*, a phenomenological quantity, which in the considered case of simple cubic lattice can be defined as follows:

$$M_n = \mu_n / a^3. \tag{6}$$

Then, (5) becomes:

$$\vec{h}_{n'} = \frac{1}{4\pi}\sum_n D_{n,n'}\left[\hat{i}M_n^x + \hat{j}M_n^y - 2\hat{k}M_n^z\right]. \tag{7}$$

It should be remembered that site (0, 0, n) is excluded from the sums appearing in the equation (4). Up to now, the direction of dipole arrangement has not had much importance in our reasoning. Now we shall consider the case with dipoles arranged along the z-axis only.

3. In this paragraph we shall consider a magnetic prism placed in a static magnetic field, H_0, applied along the z-axis (Fig. 1). Field H_0 is assumed to be strong enough to arrange *all* the magnetic moments along the z-axis. Then, the magnetization vector can be regarded as a superposition of two components (Fig. 1): static (parallel to the z-axis) and dynamic (lying in the (x, y)-plane):

$$\vec{M_R} = M_S\hat{k} + \vec{m_R}\ ; \tag{8}$$

M_S is the static magnetization, assumed to be homogeneous throughout the sample, and vector $\boldsymbol{m}$ denotes the dynamic magnetization, perpendicular to $\boldsymbol{M_S}$. Similarly, the dipole field, $\boldsymbol{h_{n'}}$, can be resolved into two components: static, $\boldsymbol{h_{n'}^s}$ (parallel to the z-axis), and dynamic, $\boldsymbol{h_{n'}^d}$ (lying in the (x, y)-plane):

$$h_{n'} = h_{n'}^s + h_{n'}^d\,. \tag{9}$$

These two components of the dipole field can be easily found from (7). By replacing the third component of the magnetization vector with the static magnetization (*i.e.* by putting $M_n^z \equiv M_S$, and the two other components, M_n^x and M_n^y , with the respective components of the dynamic magnetization, m_n^x and m_n^y , the following formulae are obtained:

$$\vec{h}_{n'}^s = -\left[\frac{1}{2\pi}\sum_n D_{n,n'}\right] M_S\hat{k}\,, \tag{10}$$

$$\vec{h}^{d}_{n'} = \frac{1}{4\pi}\sum_{n} D_{n,n'}\vec{m}_{n} \,, \tag{11}$$

element $D_{n,n}$ being defined by (4).

The magnetic moment dynamics is described by the phenomenological Landau-Lifshitz equation (LL):

$$\frac{\partial \vec{M}_{R}}{\partial t} = \gamma\mu_{0}\vec{M}_{\vec{R}} \times \vec{H}_{\mathrm{eff},\vec{R}} \,, \tag{12}$$

$H_{\mathrm{eff},\vec{R}}$ denoting the effective magnetic field acting on the magnetic moment in site R. This effective field is a superposition of two terms only: the applied field, H_0, and the field $h_{n'}$ produced by the magnetic dipole system:

$$H_{\mathrm{eff},\vec{R}} \equiv H_{\mathrm{eff},n'} = H_0 + h_{n'} \,. \tag{13}$$

Considering (9), we can write further:

$$H_{\mathrm{eff},n'} = \left(H_0 + h^{s}_{n'}\right)\hat{k} + h^{d}_{n'} \,; \tag{14}$$

the above-introduced dipole field components (static and dynamic) being defined by (10) and (11).

The LL equation becomes:

$$\frac{\partial m_{n'}}{\partial t} = \gamma\mu_{0}\left(M_{S}\hat{k} + \vec{m}_{n'}\right) \times \left(\left(\vec{H}_{0} + h^{s}_{n'}\right)\hat{k} + \vec{h}^{d}_{n'}\right) \,. \tag{15}$$

We shall solve it using the linear approximation, *i.e.* neglecting all the terms with m squared. Assuming the standard harmonic time-dependence of the solutions: $m_{n'} \sim e^{-i\omega t}$, (15) becomes:

$$i\Omega\vec{m}_{n'} = \hat{k} \times \left[\vec{m}_{n'}\left(\Omega_{H} - 2\sum_{n} D_{n,n'}\right) - \sum_{n} D_{n,n}\vec{m}_{n}\right] \,, \tag{16}$$

Ω and Ω_H denoting the *reduced frequency* and the *reduced field*, respectively, defined as follows:

$$\Omega \equiv \frac{4\pi\omega}{\gamma\mu_{0}M_{S}} \quad \text{and} \quad \Omega_{H} \equiv \frac{4\pi H_{0}}{M_{S}} \,. \tag{17}$$

Two complex variables are now introduced for convenience:

$$m^{\pm}_{n} = m^{x}_{n} \pm i m^{y}_{n} \,; \tag{18}$$

with these new variables, (16) splits into two independent *identical* scalar equations for m^{+}_{n} and m^{-}_{n}; this means we are dealing with magnetostatic waves polarized *circularly*. Therefore, it is enough to consider only one of these two equations, *e.g.* that for m^{+}_{n}:

$$\Omega m^{+}_{n'} = m^{+}_{n'}\left(\Omega_{H} - 2\sum_{n} D_{n,n'}\right) - \sum_{n} D_{n,n} m^{+}_{n} \,. \tag{19}$$

The above equation can be rewritten as follows:

$$\Omega m_{n'}^{+} = m_{n'}^{+}\left(\Omega_H - 2\sum_{n} D_{n,n'} - D_{n',n'}\right) - \sum_{n\neq n'} D_{n,n} m_{n}^{+}. \tag{20}$$

Note that, according to the assumption made at the beginning of this paragraph, the eigenvalues Ω (being reduced frequencies) correspond to magnetostatic waves propagating in the direction of the applied field, *i.e. along the central axis* shown in Fig. 1.

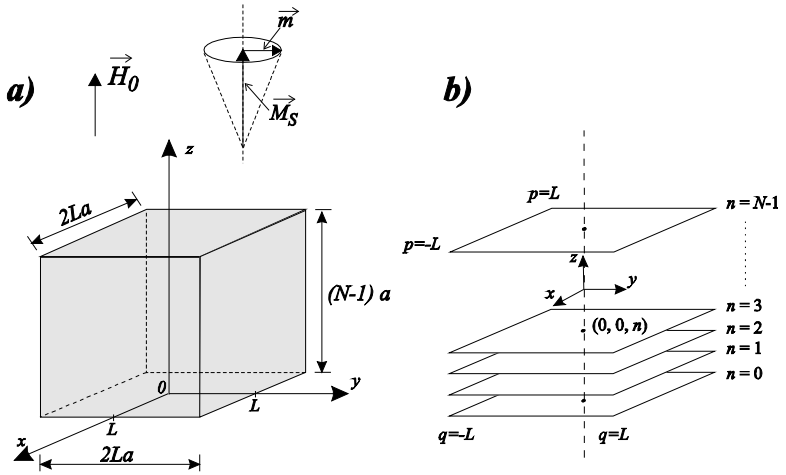

Fig. 1. (a) The prism sample considered here; the case in which the applied field, H_0, sets the magnetic moments in the direction perpendicular to the prism base (*i.e.* along the *z*-axis). The prism "thickness" is (N 1)a, and the square base side width is 2La (a denoting the lattice constant). The magnetostatic waves are assumed to propagate along the *z*-axis (*i.e.* in the direction of the applied field). (b) The planar prism model used in our calculations; the dipolar field entering the equation of motion is calculated numerically along the central *z*-axis

In the remaining part of our work we will be considering only the cubic-shaped samples, *i.e.* starting from this point we always assume 2L N 1. We also assume particular values for $\mu_0 H_0$ = 0.2 T and M_S = 0.139 · 10^6 Am^1 (YIG magnetization) with resulting value for the reduced field Ω_H = 14.374. However, we have to emphasis that selection of this particular value for Ω_H is not essential for results to be presented in subsequent sections of this work, since the distribution of eigenvalues Ω and profiles of modes associated with them are not sensitive to the choice of particular Ω_H value: the particular value of Ω_H only sets the *whole* spectrum in a given frequency region and if Ω_H changes the whole spectrum is shifted to another region, but the *relative* distribution of mode eigenfrequencies remains unchanged.

4. We shall investigate magnetostatic excitations in a cube of size 40a (a being the lattice constant). The cube consists of 41 planes normal to the *z*-axis and numbered with index n, ranging from n = 0 (the left face) to n = 40 (the right face). The effective dipole field calculation procedure applied in the previous paragraphs allows to find the field in *z*-axis points only, *i.e.* along the cube *central axis*, passing through opposite cube face centers; this is

the idea of the approximation used throughout this study, and henceforth referred to as *central-axis approximation* (CAA). With these assumptions, the problem of motion − to be solved on the basis of (20) − reduces to a single dimension in the space of variable n; the domain of the investigated motion is the interval $\tilde{n} \in (0, N-1)$, between two opposite cube face centers.

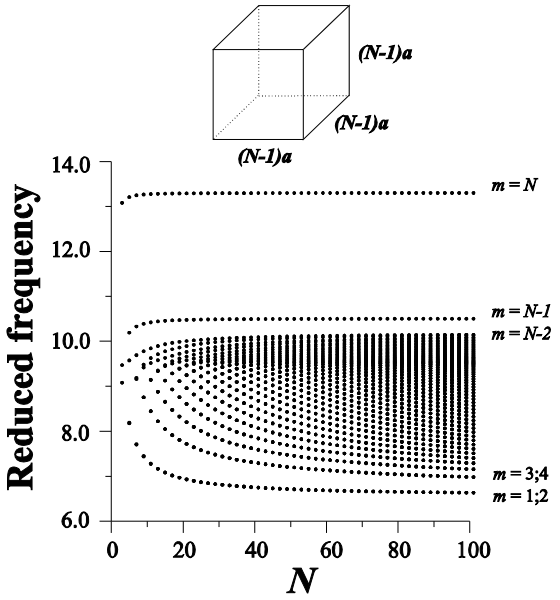

Fig. 2. The quantized magnetostatic mode frequencies *vs*. the cube size, N; m indicates the mode number

Figure 2 presents the discrete spectra of numerically calculated magnetostatic mode frequencies in a cube of variable size; the spectrum evolution with increasing N, or cube size, is visualized by the depicted frequency branches, each corresponding to one mode of a fixed number m. The plot shows clearly that only in the lowest N value range ($N < 50$) the frequency spectrum changes in a significant way; above this range, the frequency values stabilize at levels independent of N. A striking feature is that the frequencies of the two highest modes, $m = N-1$ and $m = N$, as well as those of the two lowest ones, $m = 1$ and $m = 2$, are pronouncedly separated from the rather uniform "band" formed by the other mode frequencies. In Figure 3, showing $|m^+|$ mode profiles in a $40a \times 40a \times 40a$ cube, these "detached" modes reveal quite distinct amplitude distributions, differing from those of the other modes: modes $m = N-1$ and $m = N$ appear to be of the *bulk-extended* (BE) type (with antisymmetrical and symmetrical amplitude distribution, respectively), whereas modes $m = 1$ and $m = 2$ are *surface-localized* (SL), the lower one being *antisymmetrical*, and the higher one *symmetrical*. All the other modes, within the "band", can be qualified as *localized* (*L*), their maximum amplitudes localizing in some specific regions inside the sample; as these localization regions are found to vary with the mode number, the mode localization appears to depend on the mode frequency.

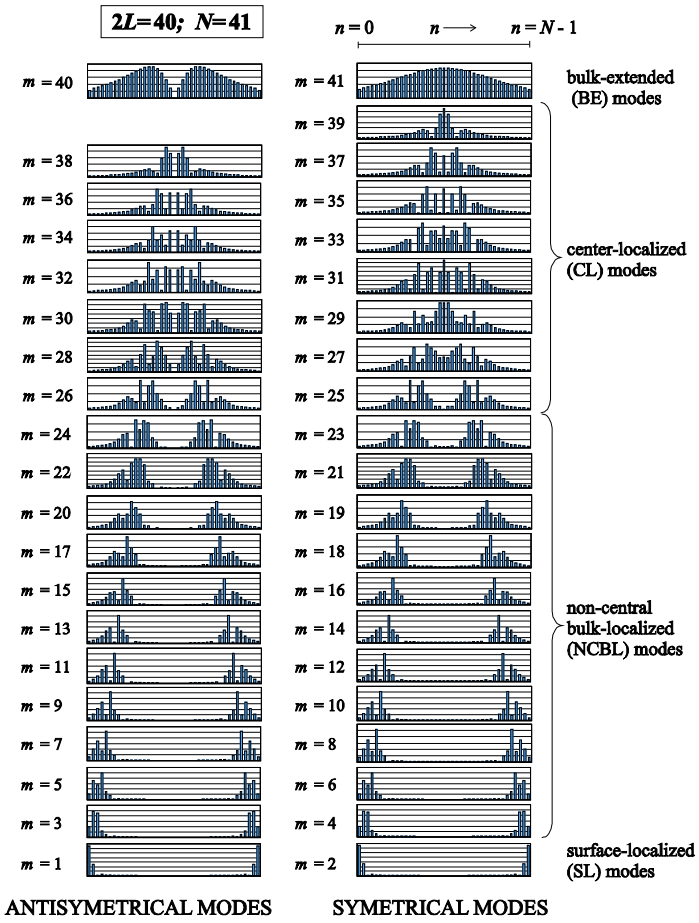

Fig. 3. Numerically calculated magnetostatic mode $|m^+|$ profiles in a cubic sample of edge size $40a$; the profiles are depicted along the central axis (indicated in Fig. 1). The modes are divided here into symmetrical (right column) and antisymmetrical (left column) groups. The localized modes can be regarded as a family consisting of three mode localization types: *central-bulk*, *non-central* and *surface* localization

To examine this relation in detail, let's note that the band modes can be divided into two groups: modes $m = 3\dot{2}4$ and $m = 2\dot{5}39$, showing different localization regions. A characteristic feature of the first-group modes is a zone of *zeroing* amplitudes around the sample center; *two* non-zero amplitude regions are present at both sides of the central "dead" zone with amplitudes reaching a maximum at a certain point. The localization reaches the sample center for the modes of the other group (*i.e.* $m = 2\dot{5}39$); typical for this group, the central localization region tightens around the sample center as mode energy increases. With respect to the above-discussed localization properties in both groups, the second-group modes can be qualified as

center-localized (CL), and the first-group ones as *non-central bulk-localized* (NCBL) (or, alternatively, *empty-center bulk localized*).

5. Let's increase the cube size to examine its effect on the mode energy spectrum and profiles. Figure 4 presents a juxtaposition of profiles in cubes of two different sizes: $2L = 40$

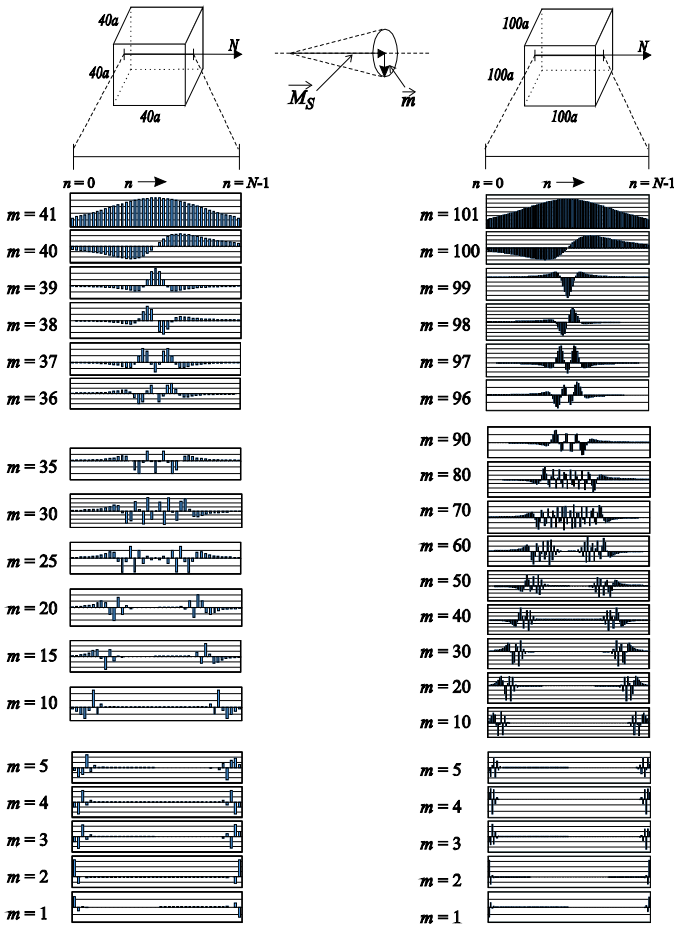

Fig. 4. Juxtaposition of magnetostatic mode profiles in two cubes of different sizes. Note that when the cube size increases, the lower modes tend to localize in the surface region, while the upper modes become strongly localized around the cube center; the two highest modes remain practically unchanged

and $2L = 100$. The profile invariance is found to be limited to the BE modes only ($m = 1; 2$) whose profiles remain unchanged in spite of the size increase. The other states reveal apparently changed localization: the NCBL modes in the $2L = 100$ cube, showing substantially larger dead regions (with respect to the $2L = 40$ cube), are practically of *sub-surface localized* (SSL) nature; in the CL modes, the localization zone has tightened around the strict sample center. Thus, we can anticipate that further size increase shall result in a deepening of

the above-mentioned localization changes, and that consequently, the magnetostatic mode spectrum in large cubic samples shall consist of three clearly different mode groups: (a) two highest-frequency *bulk-extended modes* (AS and S), (b) *center-localized modes* with intermediate frequencies, and (c) lowest-frequency *surface-localized modes*.

A problem to be solved next is the mode localization behaviour when the sample is "deformed", losing its cubic symmetry. Another question requiring future investigation is the mode localization dependence on mode propagation direction. In another study we are going to examine magnetostatic modes propagating *perpendicularly* to the applied field.

Acknowledgements

This work was supported by the Polish Committee for Scientific Research through the projects KBN-2P03B 120 23 and PBZ-KBN-044/P03-2001.

References

[1] D. Shi, B. Aktas, L. Pust, and F. Mikailov, *Nanostructural Magnetic Materials and Their Applications*, Lectures notes in physics: Vol. 593; (Springer-Verlag, Berlin 2002).
[2] D. V. Berkov, N. L. Gorn, and P. Görnert, phys. stat. sol. (a) **189**, 409 (2002).
[3] S. Tamaru, J. A. Bain, R. J. M. van de Veerdonk, T. M. Crawford, M. Covington, and M. H. Kryder, J. Appl. Phys. **91**, 8034 (2002).
[4] R. Damon and J. Eshbach, J. Phys. Chem. Solids **19**, 308 (1961).
[5] H. J. G. Draaisma and W. J. M. de Jonge, J. Appl. Phys. **64**, 3610 (1988).